



Simplified Evaluation of the Additional Shear Demand Due to Masonry Infills

Fabio Di Trapani¹(✉), Valentina Bogatkina², Marilisa Di Benedetto¹, Antonio Pio Sberna¹, Massimo Petracca², and Guido Camata³

¹ Dipartimento di Ingegneria Strutturale, Edile e Geotecnica,
Politecnico di Torino, 10129 Turin, Italy
fabio.ditrapani@polito.it

² ASDEA Software Technology, Via Alide Breviglieri 8, Pescara, Italy

³ Department of Engineering and Geology, University of Chieti-Pescara
“G. D’Annunzio”, Pescara, Italy

Abstract. Masonry infills enclosed in reinforced concrete (RC) frames exert a significant stiffening and strengthening action that can result favorable or adverse in the case earthquake-induced loads. The force increment is transferred to the RC frame column ends as an additional shear force, potentially causing local shear failures at the end of the columns. The additional shear demand due to masonry infills cannot be evaluated by the common equivalent strut models. On the other hand, refined finite element models are not computationally effective to be used in practice. With the aim to maintain the simplicity of the equivalent strut approach without losing the information about the actual shear force on the columns, this paper presents a detailed study about the infill-frame shear transfer mechanism. Refined 2D nonlinear models of real experimental tests on infilled frames have been defined using the OpenSees / STKO software platform. Shear demands on the columns are extracted by integrating the nodal forces at specific section cuts of the RC members. The same simulations are made using the equivalent strut approach. An analytical relationship is finally proposed to estimate the additional shear demand at the ends of the columns. The latter relates the additional shear demand to the current axial force on the equivalent struts and the geometrical and mechanical properties of the infilled frames. The formula can be easily implemented to perform shear safety checks at the column ends when performing seismic assessments.

Keywords: Infilled frames · Shear · Masonry · Reinforced concrete · OpenSees · STKO

1 Introduction

Infill-frame interaction has been investigated since the middle of the previous century by researchers from all around the world. Despite the large number of available theoretical and experimental studies, the interest in this topic has never stopped over the time. This can be also observed from the intense experimental activity that has persisted even in past 10 years (Da Porto et al. [1], Cavaleri and Di Trapani [2], Bergami and Nuti [3], Verderame et al. [4], Morandi et al. [5]). Infill-frame interaction occurs both at

global and local level. Global interaction effects affect the overall resistance, stiffness, ductility, and collapse modes (Uva et al. [6]; Fiore et al. [7]; Cavaleri et al. [8], Di Trapani and Malavisi [9]). On the other hand, local interaction of infills with the frame members also occur. In fact, infill walls subject to lateral loads, partially disconnect from the frame, causing a concentrated force transfer at the ends of reinforced concrete elements (Fig. 1a), resulting in a localized increase of shear demand (Koutoumanos et al. [10]; Cavaleri and Di Trapani [11]; Calìo and Pantò [12]; Milanesi et al. [13]). The additional shear demand affects the column ends and beam-column joints, jeopardizing the development local brittle failure mechanisms (Fig. 1a–c).



Fig. 1. (a) Local shear interaction of an infilled frame; (b) Shear failure at column ends; (c) Shear failure at column ends.

2 Detailed FE Modelling of the Infilled Frames

2.1 Specimen Details

Six in-plane experimental tests on solid masonry-infilled frames were selected as benchmark tests from the experimental campaigns by Mehrabi and Shing [14] and Cavaleri and Di Trapani [2]. The specimens were chosen to provide as much coverage possible of the various masonry infill typologies. Specimens 5, 8, and 9 from Mehrabi and Shing [14] were arranged using clay hollow brick masonry (8) and solid brick masonry (5 and 9). Specimens S1A, S1B, and S1C by Cavaleri and Di Trapani [2] were arranged with calcarenite, hollow clay, and lightweight concrete units, respectively. Additionally, the aspect ratio (l/h) of the infills varied between the specimens of the two sets. The ratio l/h was, 1.43 for the specimens by Mehrabi and Shing [14] and 1.0 for the specimens by Cavaleri and Di Trapani [2]. The specimens' characteristics are reported in Table 1.

Table 1. Specimens' details.

Reference	Spec	Masonry type	Infill length (l) [mm]	Infill height (h) [mm]	Aspect ratio (l/h) [-]	Load on columns [kN]
Mehrabi & Shing [14]	5	Solid clay bricks	1600	1600	1.0	294
	8	Holl. Clay bricks	1600	1600	1.0	294
	9	Solid clay bricks	1600	1600	1.0	294
Cavaleri & Di Trapani [2]	S1A	Solid calcarenite units	2032	1422	1.43	200
	S1B	Holl. Clay blocks	2032	1422	1.43	200
	S1C	Holl. LW conc. Units	2032	1422	1.43	200

2.2 Detailed FE Modelling of the Specimens with OpenSees/STKO

The STKO software platform [15] for OpenSees [16], was used to carry out refined 2D continuum micro-modelling of the experimental tests. Masonry units and mortar were modelled in detail as separate continuous parts (Fig. 2a). The *DamageTC3D* constitutive model (Petracca et al. [17]) was applied to all of the 2D elements (concrete, masonry units and mortar). The latter is based on continuum damage mechanics, which implies the following tension-compression damage framework:

$$\sigma = (1 - d^+) \bar{\sigma}^+ + (1 - d^-) \bar{\sigma}^- \quad (1)$$

where σ is the nominal stress tensor, while $\bar{\sigma}^+$ and $\bar{\sigma}^-$ are the positive and negative parts of the effective stress tensors, respectively. The damage indices for the material in tension and compression are denoted by the letters d^+ and d^- , respectively. They are scalars assuming values between 0 and 1.

Rebars were modelled using the *Steel02* uniaxial material model as 2D fiber-section components. Rebars were joined to the 2D concrete frame with the aid of the embedded contact element (*ASDEmbeddedNodeElement*) (Fig. 2c). An interaction between concrete and rebars with node-to-element links is defined to simulate this type of contact. In this case, the reinforcement has constrained nodes, whereas the concrete has retained nodes. The condition must be applied to this interaction with a penalty parameter. The constraint of that contact was enforced by the application of a penalty stiffness value. The interface between the RC frame and the infill wall was created by first assigning a node-to-node interaction (Fig. 2b), and then simulating the contact and frictional response of the interface using the *ZeroLengthImplexContact* element. The normal and tangential interface stiffness were calibrated starting by suitable literature values. The friction coefficient was assumed as 0.7.

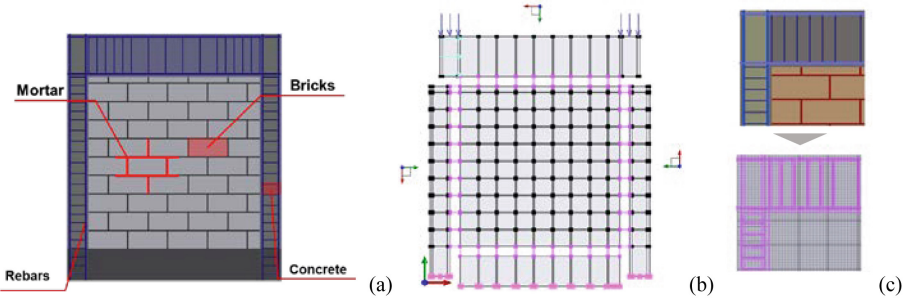


Fig. 2. Refined FE Micro-model of the infilled frame in OpenSees/STKO: (a) Element subdivision; (b) Modelling of frame-infill the interface; (c) Geometric layout of reinforcement and Node-to-element links (connection between rebars and frame).

2.3 Analysis and Model Validation

The analyses were carried out in two steps. First vertical loads were applied at the top of the columns. Subsequently, a horizontal monotonic displacement pattern is applied. In Fig. 3, the lateral force vs. lateral displacement response from the micro-models are compared to the positive and negative experimental monotonic envelopes. As it can be observed the latter show a good agreement in terms of peak resistance, stiffness, and post-peak decay.

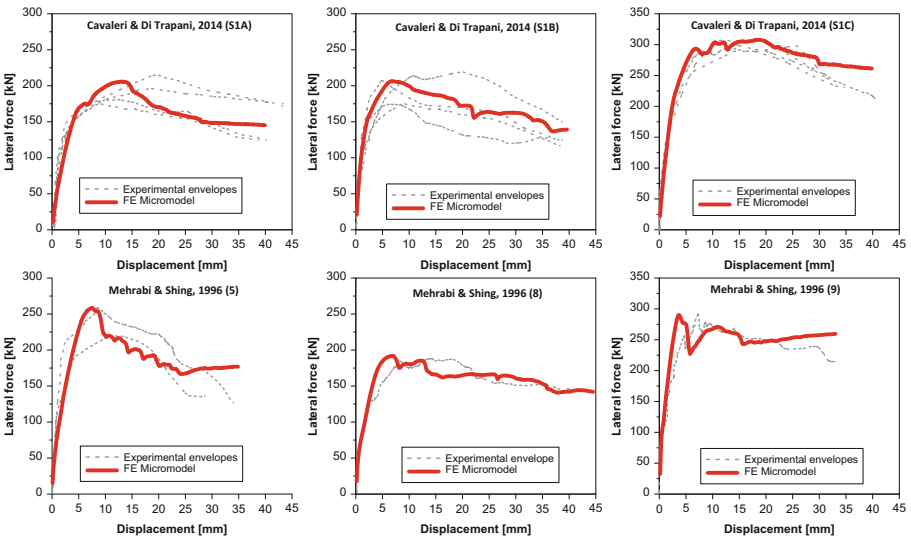


Fig. 3. Comparisons between experimental responses and numerical FE simulations.

In Fig. 4, experimental and numerical damage patterns are also compared. The numerical model was also able to accurately predict the main cracking patterns in the masonry (bricks cracking and mortar joints sliding) as well as reinforced concrete members shear and flexural damage.

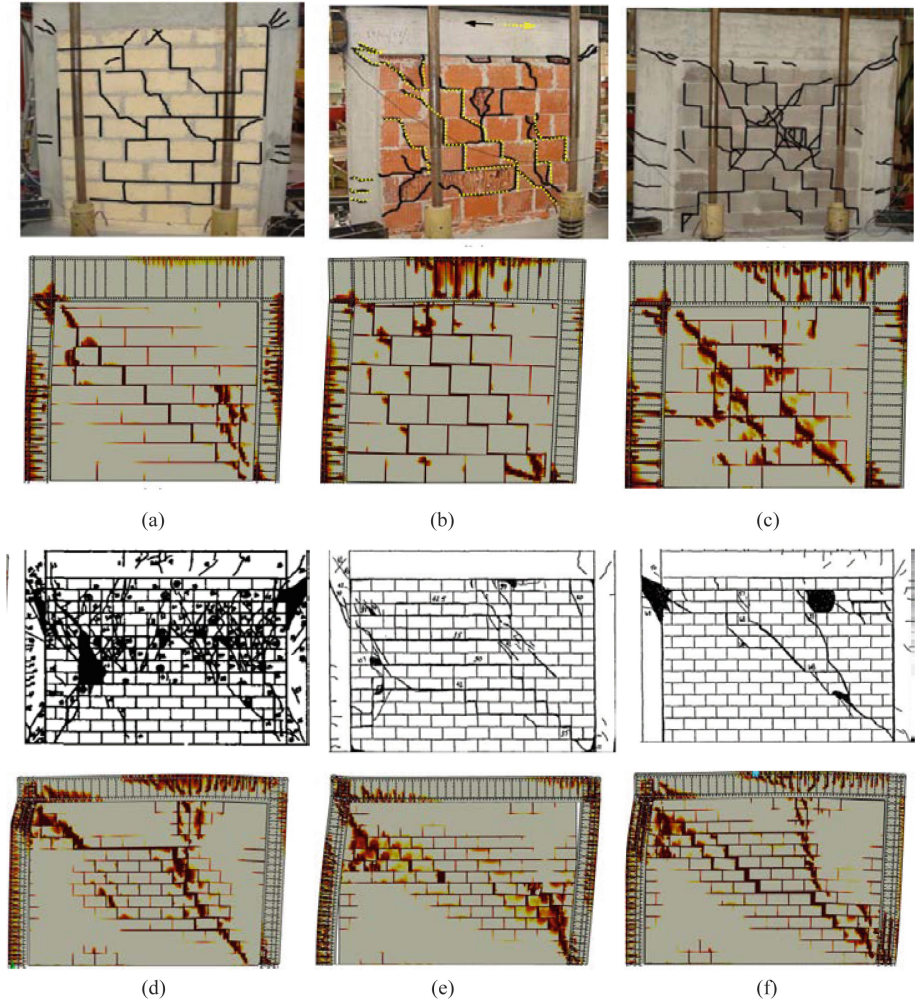


Fig. 4. Comparison between experimental and numerical damage patterns for Cavaleri & Di Trapani [2] specimens: (a) S1A; (b) S1B; (c) S1C and Mehrabi & Shing [14] specimens: (d) 5; (e) 8; (f) 9.

3 Assessment of the Additional Shear Demand at RC Columns Ends

Shear demand at the column ends of an infilled frames highly increases at the ends because of the normal stresses locally transferred by the infill to the column (Fig. 5). Because of this interaction, the shear diagram assumes a cubic trend in these areas (Cavaleri and Di Trapani [11]), raising some uncertainties about the reference value to consider as the nominal shear demand at the ends. To circumvent this uncertainty, the reference shear demand was here conventionally taken as the average of the shear demand values obtained from three section cuts made at the ends and in the middle of a critical region having an extension of $1.5 h_c$ (h_c being the height of the column cross section, Fig. 5). The internal forces were extracted from the numerical model by a TCL script that allows to collect the internal forces and integrate them along the section cuts.

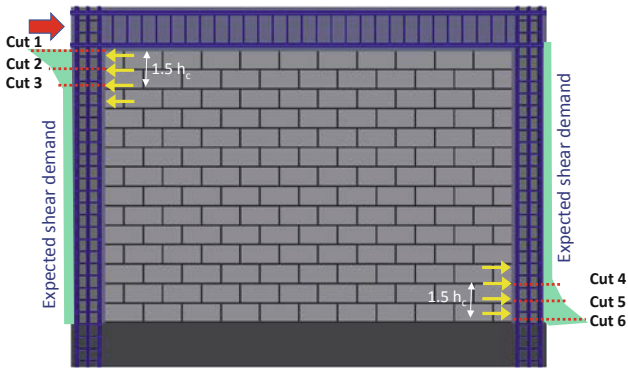


Fig. 5. Expected shear demand trend at the columns of an infilled frame and identification of the section cuts.

The results of this process are shown in Figs. 6 and 7, where the leeward and windward columns' section cut shear forces are illustrated. In Figs. 6 and 7, average trends are also shown. It is noteworthy observing that shear demands are significantly different at the ends of windward and leeward columns for infilled frames with an aspect ratio of 1. Conversely, they are quite similar in the cases of rectangular infilled frames. It should be finally noted that the average shear demand roughly corresponds to the shear demand in the middle cross sections (Cuts 2 and 5).

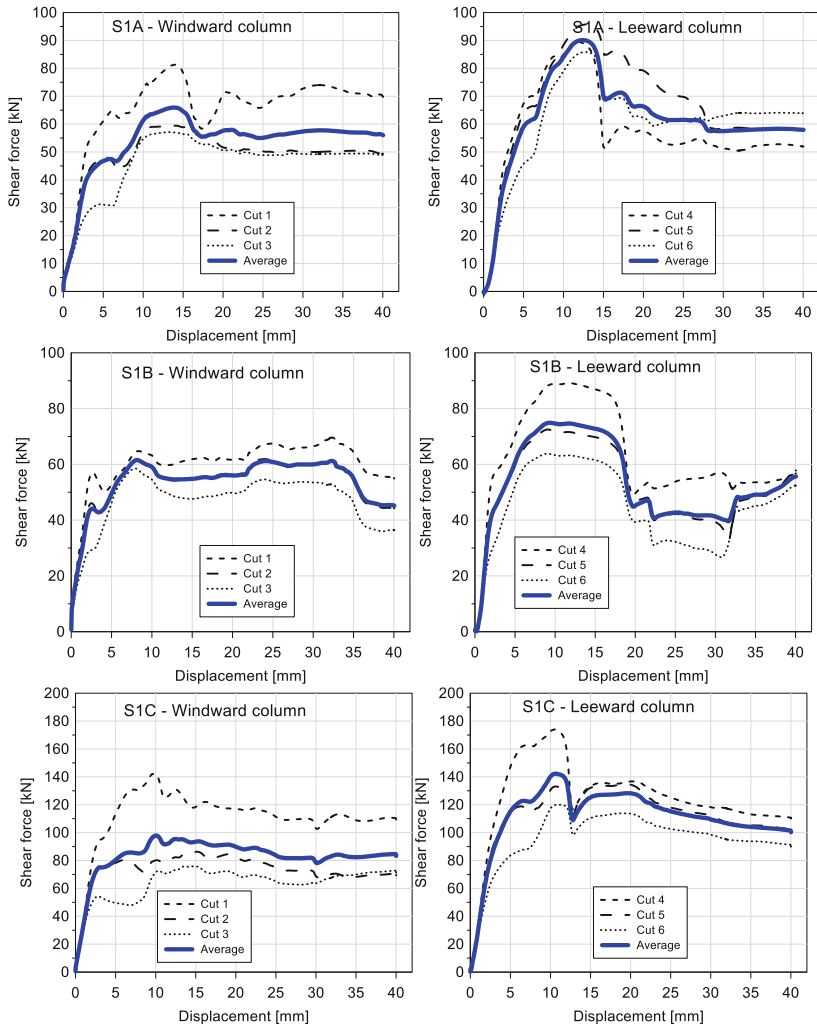


Fig. 6. Total shear demand at the windward and leeward column ends for Cavaleri & Di Trapani [2] specimens.

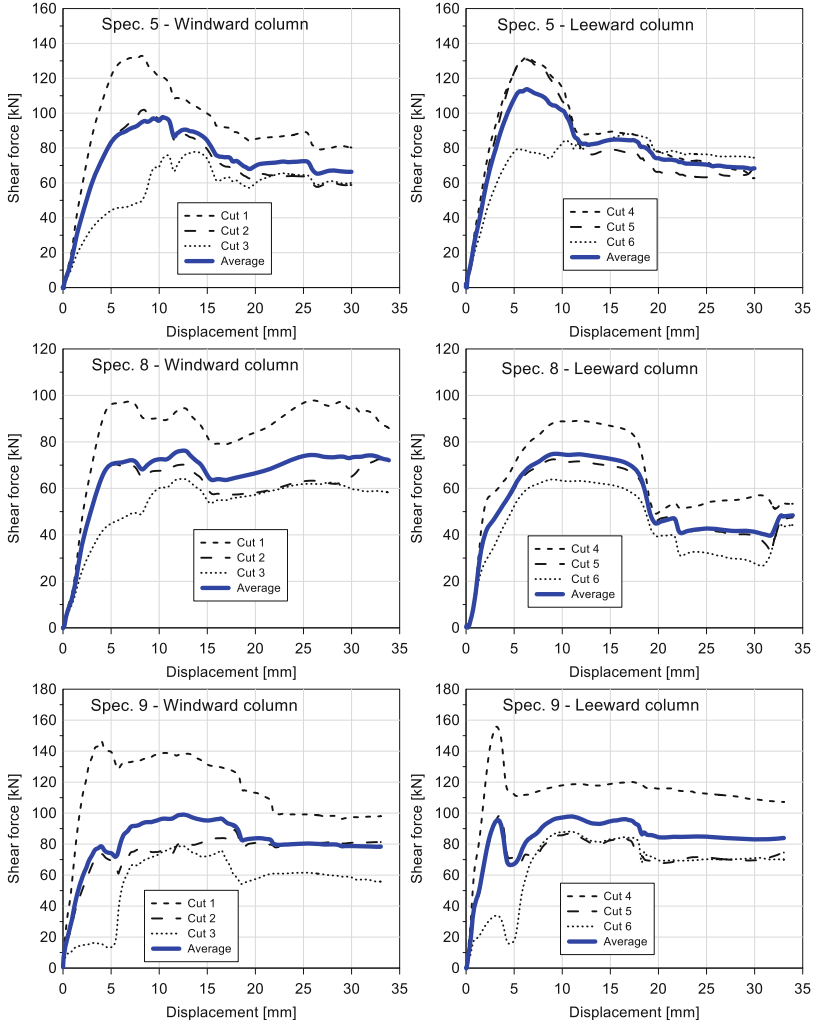


Fig. 7. Total shear demand at the windward and leeward column ends for Mehrabi & Shing [14] specimens.

4 Evaluation of the Additional Shear Demand Using Macro-modelling Approach

Equivalent strut macro-models do not allow assessing local shear demand due to frame-infill interaction. Nevertheless, considering Fig. 8a it is possible to suppose that the total shear demand at the end of a column adjacent to the infill ($V_{d,tot}$) can be decomposed as the sum of the drift-related shear on the frame ($V_{d,frame}$) and of the additional shear demand due to frame-infill interaction ($V_{d,inf}$), that is:

$$V_{d,tot} = V_{d,frame} + V_{d,inf} \quad (2)$$

While $V_{d,frame}$ is already available as shear internal force from the frame, the term $V_{d,inf}$ is unknown. However it can be reasonably assumed the shear force $V_{d,inf}$ is a rate of the axial force acting on the equivalent strut. In fact, considering the forces acting on a portion of infill at the end of a column (Fig. 8b), the translational equilibrium equation provides:

$$V_{d,inf} = N \cos \theta - T \quad (3)$$

which means that the additional shear demand is the difference between the horizontal component of the axial force on the equivalent strut and the tangential friction force at the interface (T). The latter is related to the vertical component (σ_v) of the normal stress acting on the strut (σ_n) through the friction coefficient (μ) and acts on a contact length (αl), that is a portion of the total length of the infill (αl , with $\alpha \leq 1$). The tangential force at the interface is therefore as:

$$T = \mu \cdot \sigma_v \cdot t \cdot \alpha l \quad (\sigma_v = \sigma_n \sin \theta; \sigma_n = N/w \cdot t) \quad (4)$$

w and t being the width and the thickness of the equivalent strut. Substituting Eq. (4) in Eq. (3) one obtains:

$$V_{d,inf} = N \cos \theta - \mu \sigma_n \sin \theta \cdot t \cdot \alpha l = N \cos \theta - \frac{\mu \cdot N \sin \theta \cdot t \cdot \alpha l}{w \cdot t} = N \left(\cos \theta - \frac{\mu \cdot \sin \theta \cdot \alpha l}{w} \right) \quad (5)$$

The additional shear demand is evaluated as a function of the contact length αl and the current axial force on the equivalent strut. In order to validate the reliability of Eq. (2) coupled with Eq. (6), the above described specimens were modelled using the macro-modelling method suggested by Di Trapani et al. [18], and in consideration of the additional findings from [19–24].

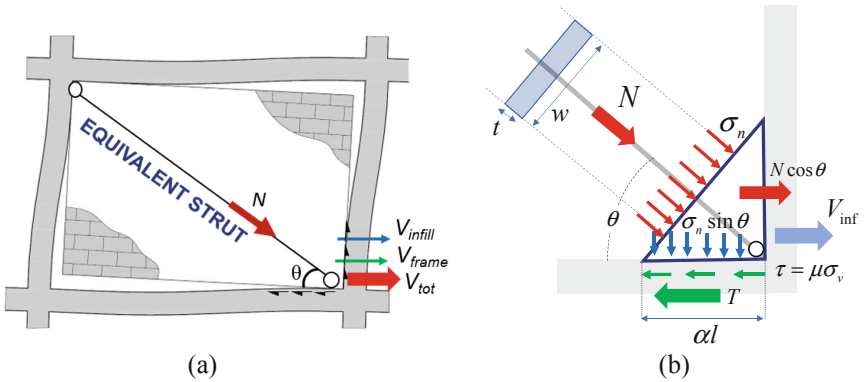


Fig. 8. (a) Decomposition of shear demand at the end of the columns of an infilled frame (b) Force transfer due to frame-infill interaction.

Results obtained from the application of the proposed analytical approach, correcting the shear demand obtained from the macro-model are illustrated in Figs. 9 and 10. A noticeable consistency with the results from the refined micro-model is observed despite the simplicity of the analytical formulation. Regarding the contact length, it was estimated that for the windward and leeward columns, $\alpha l = 0.30 \cdot l$ and $0.4 \cdot l$ for $l/h = 1$, and $\alpha l = 0.25 \cdot l$ and $0.3 \cdot l$ for $l/h = 1.5$, respectively.

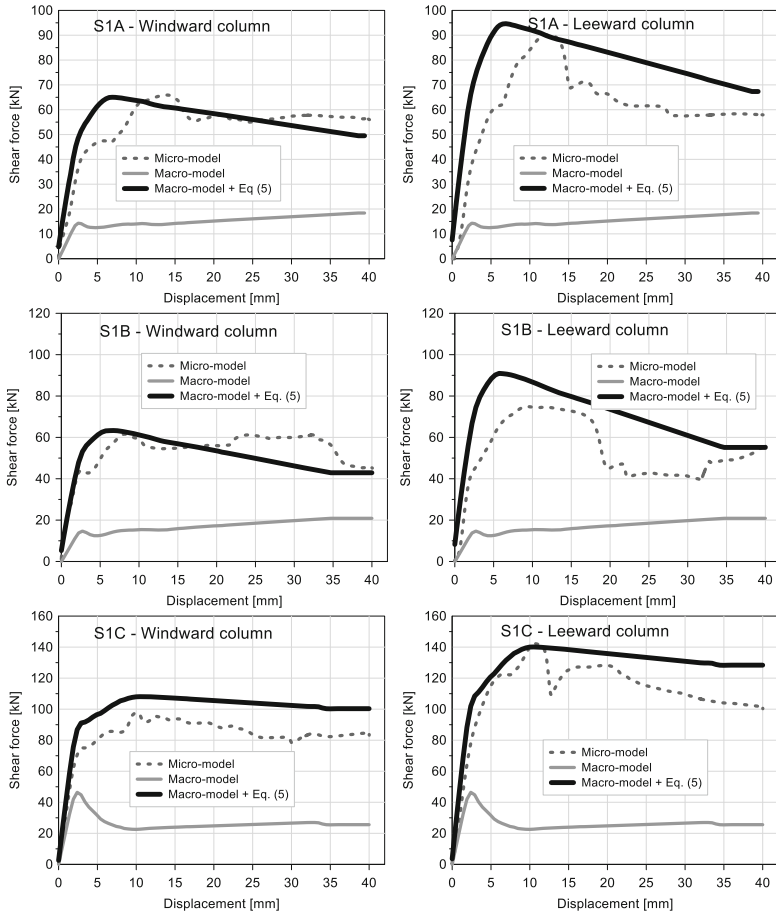


Fig. 9. Comparison between macro-model and micro-model predictions of total shear demand at the windward and leeward column ends for Cavaleri & Di Trapani [2] specimens: S1A; S1B; S1C.

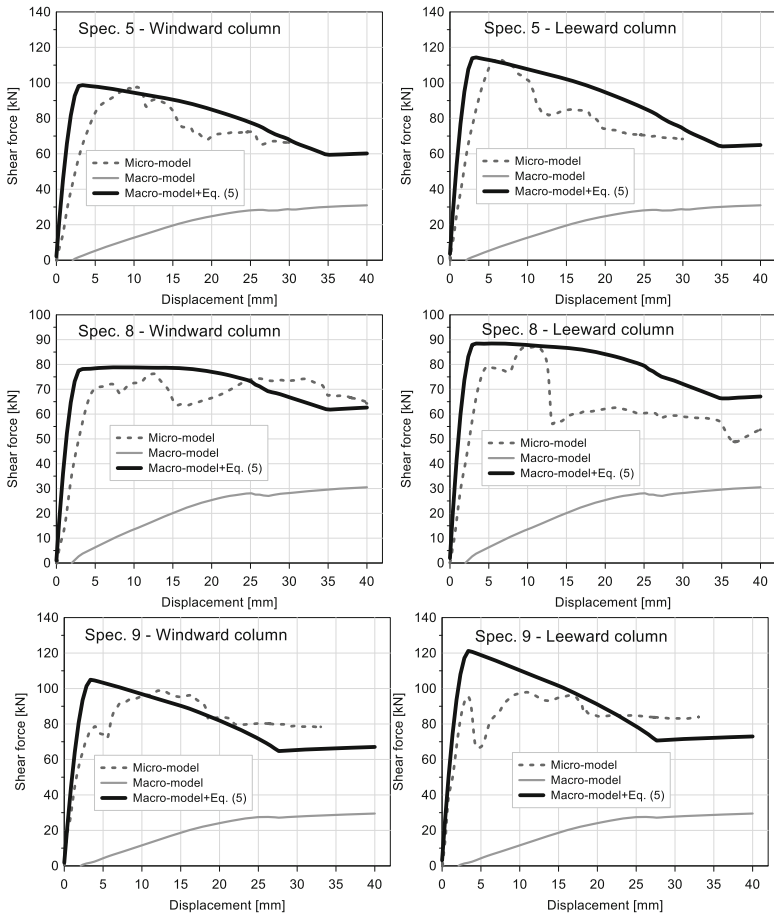


Fig. 10. Comparison between macro-model and micro-model predictions of total shear demand at the windward and leeward column ends for Mehribi & Shing [14] specimens: 5; 8; 9.

5 Conclusions

Assessment of the additional shear demand due to the frame-infill interaction cannot be neglected, especially when assessing substandard existing reinforced concrete buildings. The paper presented a numerical investigation of six infilled frame specimens subject to in plane loads which were already experimentally tested in previous studies. A refined micromodel realized with OpenSees/STKO, was used to determine the additional shear demand at the end of the columns of these specimens. Subsequently, an analytical formulation was proposed to estimate the additional shear demand using the quite simple and popular equivalent strut approach. Results have demonstrated that the additional shear demands at the column ends depends on the effective contact length of the infill with the frame (αl) as well as the current axial force on the equivalent strut. Assuming contact length values in the range of $0.25l-0.40l$, the preliminary

comparisons of the shear demand evaluated by the micromodel with that of the micromodel corrected by the proposed equation, produced satisfactory results. The proposed strategy keeps all the benefits of employing the simple equivalent strut technique while enabling accurate real-time shear safety checks at the columns' ends. More research is needed to provide accurate values for the contact lengths with a general validity and to validate the proposed approach using a larger dataset of experimental tests.

References

1. da Porto, F., Guidi, M., Dalla Benetta, N., Verlato, F.: Combined in-plane/out-of-plane experimental behaviour of reinforced and strengthened infill masonry walls. In: Proceedings of the 12th Canadian Masonry Symposium, June 2–5, Vancouver, Canada (2013)
2. Cavaleri, L., Di Trapani, F.: Cyclic response of masonry infilled RC frames: experimental results and simplified modeling. *Soil Dyn. Earthq. Eng.* **65**, 224–242 (2014)
3. Bergami, A.V., Nuti, C.: Experimental tests and global modeling of masonry infilled frames. *Earth Struct.* **9**(2), 281–303 (2015)
4. Verderame, G.M., Ricci, P., Del Gaudio, C., De Risi, M.T.: Experimental tests on masonry infilled gravity- and seismic-load designed RC frames. In: Proceedings of 16th International Brick and Block Masonry Conference (IBMAC), Padua, Italy (2016)
5. Morandi, P., Hak, S., Magenes, G.: In-plane experimental response of strong masonry infills. *Eng. Struct.* **156**, 503–521 (2018)
6. Uva, G., Rafeale, D., Porco, F., Fiore, A.: On the role of equivalent strut models in the seismic assessment of infilled RC buildings. *Eng. Struct.* **42**, 83–94 (2012)
7. Fiore, A., Porco, F., Rafeale, D., Uva, G.: About the influence of the infill panels over the collapse mechanisms active under pushover analyses: two case studies. *Soil Dyn. Earthq. Eng.* **39**, 11–22 (2012)
8. Cavaleri, L., Di Trapani, F., Asteris, P.G., Sarhosis, V.: Influence of column shear failure on pushover-based assessment of masonry infilled reinforced concrete framed structures: a case study. *Soil Dyn. Earthq. Eng.* **100**, 98–112 (2017)
9. Di Trapani, F., Malavisi, M.: Seismic fragility assessment of infilled frames subject to mainshock/ aftershock sequences using a double incremental dynamic analysis approach. *Bull. Earthq. Eng.* **17**(1), 211–235 (2019)
10. Koutromanos, I., Stavridis, A., Shing, P.B., Willam, K.: Numerical modelling of masonry-infilled RC frames subjected to seismic loads. *Comput. Struct.* **89**, 1026–1037 (2011)
11. Cavaleri, L., Di Trapani, F.: Prediction of the additional shear action on frame members due to infills. *Bull. Earthq. Eng.* **13**(5), 1425–1454 (2014). <https://doi.org/10.1007/s10518-014-9668-z>
12. Caliò, I., Pantò, B.: A macro-element modelling approach of infilled frame structures. *Comput. Struct.* **143**, 91–107 (2014)
13. Milanese, R.R., Morandi, P., Magenes, G.: Local effects on RC frames induced by AAC masonry infills through FEM simulation of in-plane tests. *Bull. Earthq. Eng.* **16**(9), 4053–4080 (2018). <https://doi.org/10.1007/s10518-018-0353-5>
14. Mehrabi, A.B., Shing, P.B., Schuller, M.P., Noland, L.: Experimental evaluation of masonry-infilled RC frames. *J. Struct. Eng. (ASCE)* **122**(3), 228–237 (1996)
15. Petracca, M., Candeloro, F., Camata, G.: ASDEA Software STKO user manual (2017)
16. McKenna, F., Fenves, G.L., Scott, M.H.: Open System for Earthquake Engineering Simulation. University of California, Berkeley (2000)

17. Petracca, M., Pelà, L., Rossi, R., Zaghi, S., Camata, G., Spacone, E.: Microscale continuous and discrete numerical models for nonlinear analysis of masonry shear walls. *Constr. Build. Mater.* **149**, 296–314 (2017)
18. Di Trapani, F., Bertagnoli, G., Gino, D., Ferrotto, M.F.: Empirical equations for the direct definition of stress-strain laws for fiber-section based macro-modeling of infilled frames. *J. Eng. Mech.* **144**(11), 04018101 (2018)
19. Di Trapani, F., Vizzino, A., Tomaselli, G., Sberna, A.P., Bertagnoli, G.: A new empirical formulation for the out-of-plane resistance of masonry infills in reinforced concrete frames. *Eng. Struct.* **266**, 114422 (2022)
20. Ferrotto, M.F., Cavaleri, L., Di Trapani, F.: FE modeling of partially steel-jacketed (PSJ) RC columns using CDP model. *Comput. Concr.* **22**(2), 143–152 (2018)
21. Di Trapani, F., Giordano, L., Mancini, G.: Progressive collapse response of reinforced concrete frame structures with masonry infills. *J. Eng. Mech.* **146**(3), 04020002 (2020)
22. Di Trapani, F., Malavisi, M., Marano, G.C., Sberna, A.P., Greco, R.: Optimal seismic retrofitting of reinforced concrete buildings by steel-jacketing using a genetic algorithm-based framework. *Eng. Struct.* **219**, 110864 (2020)
23. Di Trapani, F., Sberna, A.P., Marano, G.C.: A new genetic algorithm-based framework for optimized design of steel-jacketing retrofitting in shear-critical and ductility-critical RC frame structures. *Eng. Struct.* **243**, 112684 (2021)
24. Di Trapani, F., Sberna, A.P., Marano, G.C.: A genetic algorithm-based framework for seismic retrofitting cost and expected annual loss optimization of non-conforming reinforced concrete frame structures. *Comput. Struct.* **271**, 106855 (2022)